increased signals for TF mRNA were observed in adventitial cells of the vascular wall and in surrounding adipose tissues after restraint stress, and the signals were stronger in aged mice than young mice (Figure 4B,D). In control epididymal fat tissues, a few adipocytes were positive for TF mRNA both in young and aged mice (Figure 4E,G). In epididymal fat tissues of the stressed mice, more numbers of adipocytes specifically expressed considerable amounts of TF mRNA, and, again, the adipocyte-specific signals for TF mRNA were stronger in aged mice than those in young mice (Figure 4F,H). We observed no specific hybridized signals for TF mRNA in vascular endothelial cells in any organs examined in the stressed mice (data not shown).

Induction of TF mRNA and antigen by restraint stress in obese mice

To investigate the effect of obesity on the stress-induced TF expression, we performed restraint experiments by using genetically obese mice and their lean counterparts and then analyzed TF mRNA expression in the tissues (Figure 5). Interestingly, 20 hours of restraint stress caused a substantial increase in TF mRNA level in livers of obese mice, which revealed degeneration to fatty liver but not in livers of lean mice. In kidneys and guts, differences in the induction of TF mRNA by stress between obese and lean mice were not so dramatic. In adipose tissues, the basal expression level of TF mRNA was 2-fold higher in obese mice than in lean mice. More importantly, the magnitude of induction of TF mRNA by stress was larger in adipose tissues of obese mice than in those of lean mice. The stress-induced TF expression in adipose tissues was analyzed at antigen level as well as by Western blotting using polyclonal rabbit antimouse TF antibody (Figure 6). Although TF antigen in the lysates of adipose tissues from lean mice was at an undetectable level, a specific band of 46 kDa corresponding to TF was detected in those of obese mice. The amount of TF antigen produced in adipose tissues dramatically increased after 20 hours of restraint stress in obese mice (Figure 6, lane 6), which was consistent with the data at mRNA level (Figure 5). This increase in the adipose-derived TF production may result in the higher procoagulant potential in obese mice than in lean mice because obese mice carry abundant adipose mass.

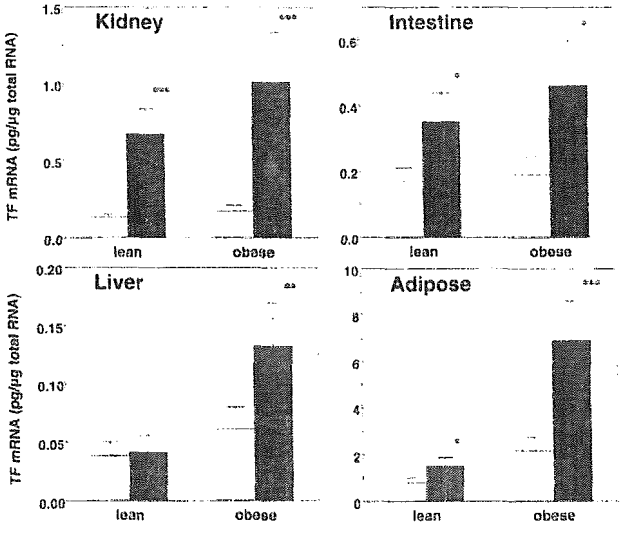

Figure 5. Induction of TF mRNA by restraint stress in obese and lean mice. Six-week-old male obese mice and their lean counterparts were stressed in restraint tubes for 20 hours. Mice were killed and the indicated tissues were removed. Total tissue RNA was prepared and analyzed for TF mRNA expression level by quantitative RT-PCR. The data are expressed as the means and SD (n = 8) in each phenotype. ▭ represents level before stress; ■, after 20 hours of restraint stress. *$P < .05$; **$P < .04$; ***$P < .02$.

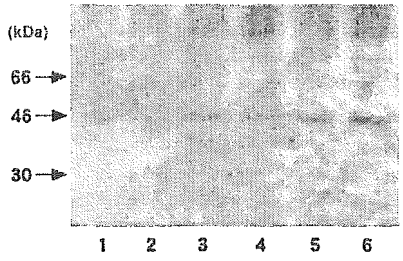

Figure 6. Western blot analysis of TF antigen in adipose tissues of the stressed obese mice. Six-week-old male obese mice and their lean counterparts were stressed in restraint tubes for 2 or 20 hours. Mice were killed and epididymal fat tissues were removed and their lysates prepared. Two micrograms of each lysate was loaded on an 8% polyacrylamide gel, and TF antigen was analyzed by Western blotting with the use of polyclonal rabbit antimouse TF antibody. Lanes 1-3, lean mice (1, no stress; 2, 2 hours of stress; 3, 20 hours of stress); lanes 4-6, obese mice (4, no stress; 5, 2 hours of stress; 6, 20 hours of stress). The numbers to the left of the blots indicate molecular weight.

Stress-induced thrombosis in aged mice and in obese mice

Microscopic examination of tissue sections revealed that renal glomerular thrombus developed in the 20-hour restraint aged (24-month-old) mice (Figure 7B) but not in the stressed young (8-week-old) mice (Figure 7A). Stress-induced thrombi formation was also observed in the microvasculature in epididymal adipose tissues in aged mice (Figure 7E) but not in adipose tissues of the stressed young mice (Figure 7D). Quantitative analysis of the stress-induced thrombi was performed by counting positive glomeruli for thrombi and the number of thrombi within the microvasculature in epididymal adipose tissues. Although renal glomerular thrombi were detected in less than 5% glomeruli in only 1 of 8 restraint mice of 8 weeks old, all (n = 8) of the stressed aged mice showed glomerular thrombi. The percentage of positive glomeruli for thrombi increased 10% to 27% (Figure 7C).[23] Similarly, we observed occasional thrombi formation in adipose tissues in 6 of 8 restraint mice 24 months old, although no thrombi were detected in adipose tissues of the stressed young mice (n = 8) (Figure 7F). Meanwhile, rare microthrombi were observed within the vasculature in adipose tissues in only 2 of 8 stressed obese mice, and none of the stressed lean mice showed thrombi formation in their adipose tissues (not shown). No stress-induced thrombi were detected in livers, hearts, intestines, and aorta of the aged mice and obese mice (not shown).

Stress-mediated changes in plasma TNF-α level and effects of anti–TNF-α antibody on the stress-induced TF mRNA

Changes in total TNF-α antigen in plasma of young and aged mice, and of obese and lean mice, by restraint stress were analyzed (Figure 8 A,D). The basal level of plasma TNF-α was already higher in aged mice versus young mice and in obese mice versus their lean counterparts. After 20 hours of restraint stress, a substantial elevation of TNF-α antigen in plasma was detected both in young and aged mice, and the magnitude of this stress-mediated induction of TNF-α was larger in aged mice (10-fold) versus young mice (4-fold). Similarly, substantial increases in plasma TNF-α level were observed in stressed obese (2.5-fold) and lean mice (4-fold).

To investigate the role of TNF-α in the induction of TF gene by stress, the mice were pretreated either with control IgG or with anti–TNF-α antibody and then subjected to restraint stress. Pretreatment of mice with anti–TNF-α antibody before restraint stress substantially attenuated the stress-induced TF mRNA expression in

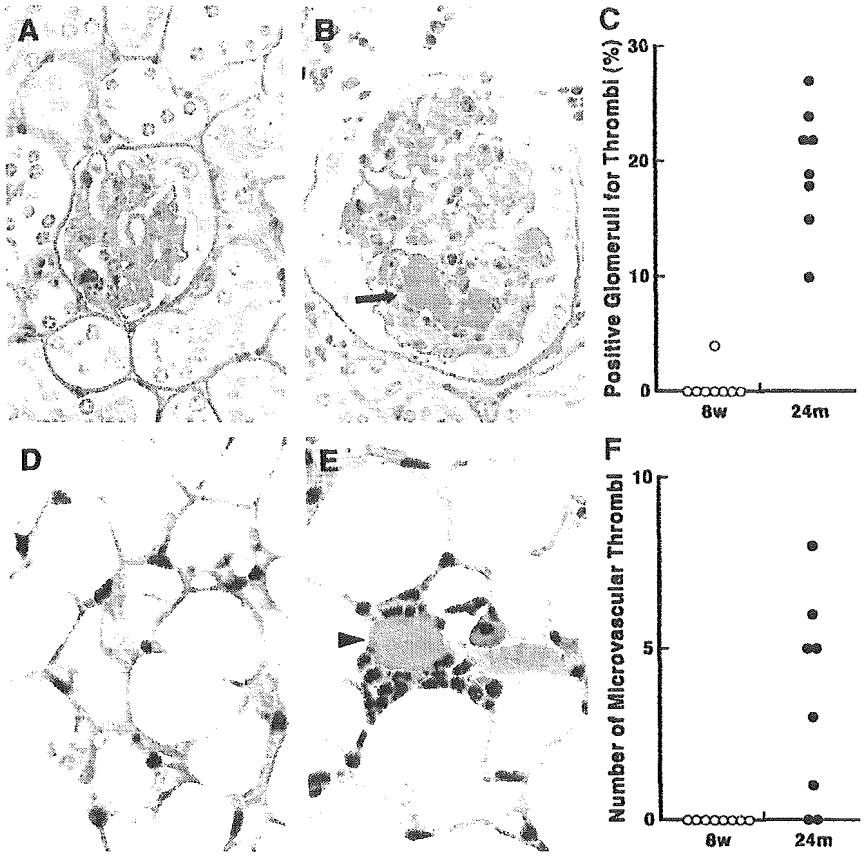

Figure 7. Stress-induced thrombi formation in tissues of young and aged mice. Renal and adipose tissues were removed from young (8-week-old) and aged (24-month-old) mice after 20 hours of restraint stress (n = 8 in each age group). Tissue sections were stained with PAS (A-B) or with hematoxylin/eosin (D-E) and examined microscopically. (A-B) Renal glomerulus of the stressed young (A) and aged (B) mice; original magnification, × 1000. An arrow denotes glomerular thrombus in aged mice. (D-E) Epididymal adipose tissues of the stressed young (D) and aged (E) mice; original magnification, × 400. An arrowhead indicates thrombi in the microvessels between adipocytes. Quantitation of stress-induced glomerular thrombi was achieved by counting the positive glomeruli for thrombi of at least 100 glomeruli in each kidney section from young (8w) and aged mice (24m), and the percentage of positive glomeruli for thrombi in each mouse is shown in panel C. Panel F shows each number of thrombi detected in the vasculature within the same size of microscopic area (90 mm^2) in epididymal fat tissues of the stressed young (8w) and aged (24m) mice.

kidneys (65%) and adipose tissues (50%), and this effect was pronounced in aged mice (Figure 8B-C). Similarly, a substantial effect of anti–TNF-α antibody on the stress-induced TF expression was observed in adipose tissues of obese mice (45%) but not in livers (Figure 8E-F). These results suggest that the induction of TF gene in adipose tissues by stress is, at least in part, mediated by endogenous TNF-α in aged mice and obese mice.

Discussion

Although hypercoagulability and thrombotic diseases appear to be induced by a variety of stress,[8-10] little information is available about underlying mechanisms. In this report, we observed that restraint stress to mice substantially induced the expression of TF gene (Figure 1). The stress-induced TF mRNA was localized primarily to renal tubular epithelial cells, adventitial cells, smooth muscle cells, and adipocytes but not to vascular endothelial cells (Figures 3-4), indicating that the induction of TF gene by stress occurs in a cell type–specific manner. It has been reported that these cells are a principal source of TF in vivo under physiologic[29] and/or pathologic conditions.[26,30] The constitutive production of TF in these cell populations suggests that TF forms a hemostatic envelope that activates the coagulation system when vascular integrity is disrupted by a variety of stressors. Another important source of TF in vivo is the adipose tissue/adipocytes.[30] The adipose tissue is a

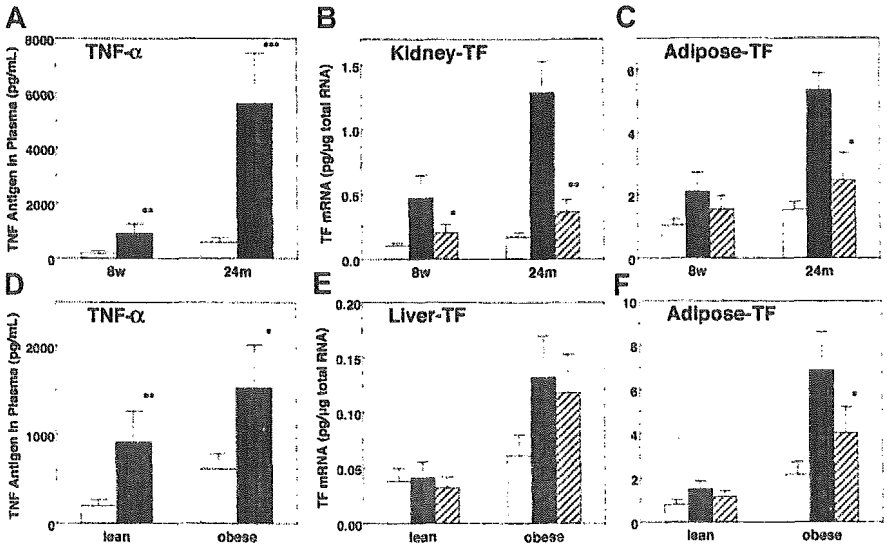

Figure 8. Changes in TNF-α antigen in plasma by stress and effects of anti–TNF-α antibody on the stress-induced TF mRNA expression. TNF-α antigen levels in plasma of 8-week-old (8w) and 24-month-old (24m) mice (A) and of 6-week-old obese and lean mice (D) before (□) and after (■) 20 hours of restraint stress were determined by enzyme-linked immunosorbent assay (*$P < .04$; **$P < .01$; ***$P < .005$). In separate experiments, the mice were pretreated either with control or with anti–TNF-α antibody (25 μg/mouse or 1 μg/g) and then subjected to 20 hours of restraint stress. Kidneys, adipose tissues, or livers were harvested and analyzed for TF mRNA by quantitative RT-PCR (young and aged mice, B and C; obese and lean mice, E and F). □ indicates no stress: ■, pretreated with control antibody; ▨, pretreated with anti–TNF-α antibody. The data are expressed as the means and SD (n = 6). Statistical significances were analyzed between the groups of pretreatment with control antibody and with anti–TNF-α antibody in each tissue (*$P < .05$; **$P < .02$).

highly vascularized organ, and the adipocytes appear to be in intimate contact with vascular beds. Under stressful conditions, the integrity of the circulation is important for the lipid utilization, and TF may help to maintain this integrity in the adipose tissue.

The incidence of thrombotic diseases is increasing in aged individuals. Aged subjects may have lower tolerance to stress[2-5] and be more susceptible to thrombotic diseases caused by a variety of stressors than the young.[13,14] We previously showed that the expression of PAI-1 was also induced by restraint stress and that this response was exacerbated by aging.[23] In this study, we demonstrated the induction of TF mRNA in several tissues by restraint stress was substantially higher in aged mice than in young mice (Figures 2-4). Renal glomerular thrombosis and microthrombi formation in adipose tissues were markedly induced by stress in aged mice (Figure 7),[23] suggesting that the stress-mediated TF induction contributes to the elevation of regional procoagulant activity and to the development of thrombosis. Thus, the increased expression of TF gene in response to stress may lead to a prothrombotic state in elderly individuals who are exposed to stress.

Obesity is associated with increased incidence of thrombotic diseases and accelerated atherosclerosis. We investigated the effect of obesity on the stress-induced TF expression and observed that TF mRNA was substantially increased by restraint stress in livers and adipose tissues of obese mice (Figures 5-6). This observation leads to a speculation that obese adipocytes and degenerative hepatocytes containing abundant lipids may show an increased response to stress in the expression of TF gene. Adipocytes/adipose tissues are the principal sites of TF production in obesity[30]; thus, obese animals may have a large potential of TF synthesis in response to stress, leading to an increase in the systemic and/or regional procoagulant activity. However, the induction of TF expression by stress in livers and adipose tissues of obese mice did not directly contribute to regional thrombi formation, implying that the process of obesity-linked thrombosis includes multifactorial and complex possibilities.

The expression of inflammatory cytokines could be altered by stress, as shown in the regulation of interleukins.[31,32] We observed that the basal level of TNF-α in plasma was markedly elevated in aged mice and obese mice,[33] as well as substantial increases in the plasma level of TNF-α antigen, which may be inducibly produced by adipose tissues,[33,34] after 20 hours of restraint stress in these mice (Figure 8). TNF-α promotes a hypercoagulable state because this cytokine was shown experimentally to increase TF expression[35] by activation of AP-1 and NF-κB sites.[16,36] Especially, adipose-derived TNF-α could play a pathologic role in obesity and insulin resistance.[33] The attenuation of the stress-induced TF expression in adipose tissues by pretreatment with anti–TNF-α antibody in aged mice and obese mice (Figure 8) suggests that this cytokine plays a key role in the stress-mediated induction of TF expression in adipose tissues. Partial effects of anti–TNF-α antibody on the stress-mediated TF induction suggest that other stress-induced neurologic substances, hormones (eg, angiotensin II),[37] and growth factors (eg, transforming growth factor-β)[38] may also contribute to the induction of TF expression by stress.

In conclusion, we demonstrate that restraint stress induces the TF expression in a tissue- and cell type–specific manner in the mouse and that aging and/or obesity enhance the stress-mediated induction of TF gene. The stress-induced endogenous TNF-α may, in part, mediate the induction of TF expression, especially in aged mice. In obese mice, TF derived from adipose tissues may contribute to an increase in regional procoagulant potential, resulting in the development of microvascular thrombi. This study presents a novel finding regarding the molecular process of the stress-induced hypercoagulability and suggests that 3 factors, including stress, aging, and obesity, may be responsible for the increased risk of thrombosis as a result of the induction of TF gene.

Acknowledgments

We thank T. Thinnes, E. Yamafuji, K. Kaneko, and K. Sakakura for their expert technical assistance; and Drs K. Enjyoji and H. Kato (National Cardiovascular Center and Research Institute, Osaka, Japan) for providing rabbit antimouse TF antibody.

References

1. Minowada G, Welch WJ. Clinical implications of the stress response. J Clin Invest. 1995;95:3-12.
2. Blake MJ, Udelsman R, Feulner GJ, et al. Stress-induced heat shock protein 70 expression in adrenal cortex: an adrenocorticotropic hormone-sensitive, age-dependent response. Proc Natl Acad Sci U S A. 1991;88:9873-9877.
3. Sapolsky RM, Krey LC, McEwen BS. The neuroendocrinology of stress and aging: the glucocorticoid cascade hypothesis. Endocr Rev. 1986;7:284-301.
4. Udelsman R, Blake MJ, Stagg CA, et al. Vascular heat shock protein expression in response to stress: endocrine and autonomic regulation of this age-dependent response. J Clin Invest. 1993;91:465-473.
5. Chin JH, Okazaki M, Hu Z-W, et al. Activation of heat shock protein (hsp) 70 and proto-oncogene expression by α1-adrenergic agonists in rat aorta with age. J Clin Invest. 1996;97:2316-2323.
6. Glavin GB, Pare WP, Sandbak T, et al. Restraint stress in biomedical research: an update. Neurosci Biobehav Rev. 1994;18:223-249.
7. Bonneau RH, Sheridan JF, Feng N, et al. Stress-induced modulation of the primary cellular immune response to herpes simplex virus infection is mediated by both adrenal-dependent and independent mechanisms. J Neuroimmunol. 1993;42:167-176.
8. Malyszko J, Urano T, Takada Y, et al. Stress-dependent changes in fibrinolysis, serotonin and platelet aggregation in rats. Life Sci. 1994;54:1275-1280.
9. Raikkonen K, Lassila R, Keltikangas-Jarvinen L, et al. Association of chronic stress with plasminogen activator inhibitor-1 in healthy middle-aged men. Arterioscler Thromb Vasc Biol. 1996;16:363-367.
10. Jern C, Eriksson E, Tengborn L, et al. Changes of plasma coagulation and fibrinolysis in response to mental stress. Thromb Haemost. 1989;62:767-771.
11. Greenberg D, Ackerman SH. Genetically obese (ob/ob) mice are predisposed to gastric stress ulcers. Behav Neurosci. 1984;98:435-440.
12. Harris RB, Zhou J, Shi M, Redmann S, Mynatt RL, Ryan DH. Overexpression of agouti protein and stress responsiveness in mice. Physiol Behav. 2000;73:599-608.
13. Ciampricotti R, el Gamal MI. Unstable angina, myocardial infarction and sudden death after an exercise stress test. Int J Cardiol. 1989;24:211-218.
14. Lecomte D, Fornes P, Nicolas G. Stressful events as a trigger of sudden death: a study of 43 medico-legal autopsy cases. Forensic Sci Int. 1996;79:1-10.
15. Edgington TS, Mackman N, Brand K, et al. The structural biology of expression and function of tissue factor. Thromb Haemost. 1991;66:67-79.
16. Mackman N. Regulation of the tissue factor gene. FASEB J. 1995;9:883-889.
17. Cui M-Z, Parry GCN, Oeth P, et al. Transcriptional regulation of the tissue factor gene in human epithelial cells is mediated by Sp1 and Egr-1. J Biol Chem. 1996;271:2731-2739.
18. Wilcox JN, Smith KM, Schwartz SM, et al. Localization of tissue factor in the normal vessel wall and in the atherosclerotic plaque. Proc Natl Acad Sci U S A. 1989;86:2839-2843.
19. Warr TA, Rao LVM, Rapaport SI. Disseminated intravascular coagulation in rabbits induced by administration of endotoxin or tissue factor: effect of anti-tissue factor antibodies and measurement of plasma extrinsic pathway inhibitor activity. Blood. 1990;75:1481-1489.
20. Semerano N, Colucci M. Tissue factor in health and disease. Thromb Haemost. 1997;78:759-764.
21. Meade TW, Ruddock V, Stirling Y, et al. Fibrinolytic activity, clotting factors, and long-term incidence of ischaemic heart disease in the Northwick Park Heart Study. Lancet. 1993;342:1076-1079.

22. Balleisen L, Bailey J, Epping PH, et al. Epidemiological study on factor VII, factor VIII and fibrinogen in an industrial population. I: baseline data on the relation to age, gender, body-weight, smoking, alcohol, pill-using, and menopause. Thromb Haemost. 1985;54:475-479.
23. Yamamoto K, Takeshita K, Shimokawa T, et al. Plasminogen activator inhibitor-1 is a major stress-regulated gene: implications for stress-induced thrombosis in aged individuals. Proc Natl Acad Sci U S A. 2002;99:890-895.
24. Yanada M, Kojima T, Ishiguro K, et al. The impact of antithrombin deficiency in thrombogenesis: LPS and stress-induced thrombus formation in heterozygous antithrombin deficient mice. Blood. 2002;99:2455-2458.
25. Samad F, Uysal KT, Wiesbrock SM, Pandey M, Hotamisligil GS, Loskutoff DJ. Tumor necrosis factor α is a key component in the obesity-linked elevation of plasminogen activator inhibitor 1. Proc Natl Acad Sci U S A. 1999;96:6902-6907.
26. Yamamoto K, Loskutoff DJ. Fibrin deposition in tissues from endotoxin-treated mice correlates with decreases in the expression of urokinase-type but not tissue-type plasminogen activator. J Clin Invest. 1996;97:2440-2451.
27. Liu MA. Overview of DNA vaccines. Ann N Y Acad Sci. 1995;772:15-20.
28. Enjyoji K, Sevigny J, Lin Y, et al. Targeted disruption of cd39/ATP diphosphohydrolase results in disordered hemostasis and thromboregulation. Nat Med. 1999;5:1010-1017.
29. Drake TA, Morrissey JH, Edgington TS. Selective cellular expression of tissue factor in human tissues: implications for disorders of hemostasis and thrombosis. Am J Pathol. 1989;134:1087-1097.
30. Samad F, Pandey M, Loskutoff DJ. Tissue factor gene expression in the adipose tissues of obese mice. Proc Natl Acad Sci U S A. 1998;95:7591-7596.
31. Shizuya K, Komori T, Fujiwara R, et al. The influence of restraint stress on the expression of mRNAs for IL-6 and the IL-6 receptor in the hypothalamus and midbrain of the rat. Life Sci. 1997;61:135-140.
32. Zuo YC, Li YF, Mei L, et al. Brain interleukin-1 is involved in generation of the serum suppressive factor induced by restraint stress in mice. Neuroimmunomodulation. 1995;2:82-87.
33. Hotamisligil GS, Arner P, Caro JF, et al. Increased adipose tissue expression of tumor necrosis factor-α in human obesity and insulin resistance. J Clin Invest. 1995;95:2409-2415.
34. Kern PA, Saghizadeh M, Ong JM, Bosch RJ, Deem R, Simsolo RB. The expression of tumor necrosis factor in human adipose tissue. J Clin Invest. 1995;95:2111-2119.
35. Kirchhofer D, Tschopp TB, Hadvary P, et al. Endothelial cells stimulated with tumor necrosis factor-α express varying amounts of tissue factor resulting in inhomogenous fibrin deposition in a native blood flow system. J Clin Invest. 1994;93:2073-2083.
36. Mackman N, Brand K, Edgington TS. Lipopolysaccharide-mediated transcriptional activation of the human tissue factor gene in THP-1 monocytic cells requires both activator protein 1 and nuclear factor κB binding sites. J Exp Med. 1991;174:1517-1526.
37. Nishimura H, Tsuji H, Masuda H, et al. Angiotensin II increases plasminogen activator inhibitor-1 and tissue factor mRNA expression without changing that of tissue type plasminogen activator or tissue factor pathway inhibitor in cultured rat aortic endothelial cells. Thromb Haemost. 1997;77:1189-1195.
38. Samad F, Pandey M, Loskutoff DJ. Regulation of tissue factor gene expression in obesity. Blood. 2001;98:3353-3358.

Journal of Gerontology: BIOLOGICAL SCIENCES
2002, Vol. 57A, No. 3, B93–B98

Histone Acetyltransferase Activities of cAMP-Regulated Enhancer-Binding Protein and p300 in Tissues of Fetal, Young, and Old Mice

Qiang Li, Hengyi Xiao, and Ken-ichi Isobe

Department of Basic Gerontology, National Institute for Longevity Sciences, Aichi, Japan.

CBP, a protein that binds to cyclic adenosine monophosphate-regulated enhancer-binding protein, and homologue protein, p300, have histone acetyltransferase (HAT) activity and are important in gene transcription, although their physiological functions in vivo remain to be further elucidated. By using immunoprecipitation and HAT activity assay we have found that p300 and CBP have similar tissue patterns of HAT activities, with the highest level in the brain, a relatively high level in the lung, spleen, and heart, an intermediate level in testes and muscle, and a lower level in liver and kidney; that HAT activities of p300 and CBP are relatively stable with advancing age in most examined tissues, but in liver, muscle, and testes, the activities are attenuated with aging; and that HAT activities of p300 and CBP are high in the brain and liver of E14 fetal and newborn mice. These data suggest that the HAT activities of p300 and CBP are important for gene transcription involved in tissue-specific expression, aging, and developing processes.

CYCLIC adenosine monophosphate (cAMP)-regulated gene expression frequently involves a DNA element known as the cAMP-regulated enhancer, or CRE (1,2). Many transcription factors bind to this element, including a specific CRE-binding protein (CREB), which is activated as a result of phosphorylation by protein kinase A (1,2). Phosphorylated CREB interacts with a 265-Kda nuclear protein termed CBP (for CREB-binding protein), which bridges the CRE/CREB complex to components of the basal transcriptional apparatus (1,2). Recently it has been shown that CBP belongs to a new family of coactivators/regulators of transcription that also includes p300, an adenovirus E1A targeted nuclear protein (3–8). p300–CBP can interact with a variety of cellular and virus proteins, as well as with transcription machinery (9,10). Most proteins that bind to p300–CBP are transcription factors. In addition, p300–CBP has intrinsic histone acetyltranferase (HAT) activity that has been proved to be critical for a large number of regulated DNA-binding transcriptions (11–13). The acetylation of histones is thought to be involved in the destabilization and restructuring of nucleosomes, which is probably a crucial event in the control of the accessibility of DNA templates to transcriptional factors (14–17). A current working hypothesis is that the recruitment of coactivators with HAT activity by promoter-bound transcription factors results in the acetylation of histone residues of nearby nucleosomes, which increases the accessibility of the DNA to the transcription machinery (17–19). Furthermore, recent studies have also shown that histones are not the only substrates of p300–CBP; p53 and some basal transcription factors (TF), such as TFIIE, TFIIF, erythroid Kruppel-like factor (EKLF), and GATA-1, are also acetylated by p300–CBP (20–23). Thus it appears that p300–CBP participates in transcription by forming the scaffold that allows various classes of transcriptional regulators to interact with specific domains within the chromatin (23). The interaction of p300–CBP with numerous DNA-binding regulatory proteins integrates and transduces signals for control of the cell cycle, differentiation, DNA repair, and apoptosis (17). Hence, the regulation of p300–CBP acetyltransferase activity may represent a mechanism for the integration of diverse signaling pathways (24).

Structure and functions of p300 and CBP have been extensively studied in in vitro systems. Although p300 and CBP are greatly important in gene expression, the HAT activities of these proteins in normal tissues have never been examined. Here, we present the data of p300 and CBP HAT activities in normal tissues of young and old mice.

Methods

Animals

Male C57/BL6J mice that were either 3 or 24 months of age were obtained from the animal center of the National Institute for Longevity Science (NILS) and sacrificed by ether and bleeding. All the mice used were bred in NILS's animal center in a strictly pathogen-free environment. Several viruses were periodically checked. The tissues of kidney, heart, liver, brain, muscle (quadriceps femurs), lung, spleen, and testes were removed, excised, and immediately put into a Lysis buffer and homogenized with an electric homogenizer. The liver and the brain of C57/BL6J murine fetus (gestation 14 days), newborn (1 day), and 1-month-old

mice were also obtained and were treated as described above.

Immunoprecipitation

The freshly isolated tissues were immediately homogenized by using a Lysis buffer containing 1% Nonidet P-40, 0.5% sodium deoxycholate, 0.1% sodium dodecyl sulfate (SDS), 150 mM sodium chloride, 50 mM Tris (pH 7.4), and 20 mM phosphate buffer (pH 7.4) supplemented with 5 mM dithiothreitol, 1 mM ethylenediamine tetra-acetic acid (EDTA), and freshly prepared protease and phosphatase inhibitors—10 mM sodium fluoride, 1 mM sodium vanadate, 1 mM phenylmethylsulfonyl fluoride (PMSF) and aprotinin, leupeptin, and pepstatin at 10 μg/ml each. The tissues were kept on ice for 30 minutes and then centrifuged at 15,000 rpm by a tabletop centrifuge for 30 minutes at 4°C. The supernatants were carefully isolated and the protein concentrations were determined by the method of Bradford assay with the Bio-Rad protein assay dye reagent (Bio-Rad, Tokyo, Japan). One milligram of protein was diluted in 1 ml of RIPA buffer and precleared by using rabbit preimmune serum (Santa Cruz Biotechnology, Santa Cruz, CA) and protein-G/sepharose beads (Amersham Pharmacia Biotech, Buckinghamshire, UK) for 2 hours at 4°C. The supernatants were incubated with the specific rabbit polyclonal antibodies for CBP (Santa Cruz, A22), p300 (Santa Cruz, N-15), or a normal rabbit IgG (Santa Cruz), in the presence of protein-G/sepharose beads at 4°C overnight. The Sepharose beads were then washed five times with RIPA buffer and used for the HAT assay.

HAT Assay

For the HAT activities of p300 and CBP to be measured, immunoprecipitation from different tissues was first performed as described above; then filter binding assays were done as Ogryzko and colleagues described (11) with minor modifications. After immunoprecipitation and being washed with RIPA buffer, samples were washed twice further with HAT assay buffer containing 50 mM Tris-HCl (pH 8.0), 10% glycerol, 1 mM PMSF, 1 mM dithiothylitol, and 10 mM sodium butyrate. They were incubated at 30°C for 60 minutes in 30 μl of HAT assay buffer containing 0.25 μCi of [^{3}H] acetyl coA (2–10 Ci/mmol, 250 μCi/ml, mCi/mmol, Amersham Pharmacia Biotech, Buckinghamshire, UK) and 50 μg/ml calf thymus histone (Sigma Chemical, St. Louis, MO). After incubation, the reaction mixture was spotted onto Whatman P-81 phosphocellulose filter paper and washed four times with 0.2 M sodium carbonate buffer (pH 9.2) at room temperature. The dried filters were counted in a liquid scintillation counter. For each specific HAT activity, the data were subtracted from normal rabbit IgG. For detecting the total cellular HAT activity, the homogenate cell lysates containing 15 μg of protein were diluted with HAT assay buffer to a final volume of 30 μl. After 0.25 μCi of [^{3}H] acetyl coA and 15 μg/ml of calf thymus histone were added, the assay process was in accordance with the method stated above.

Statistical Analysis

Data are expressed as mean ± standard error of the mean. A one-way analysis of variance (ANOVA) was used to evaluate differences among age groups.

RNA Isolation and Northern Blot Analysis

Total RNA was extracted with Trizol (Invitrogen, Carlsbad, CA) from mouse tissues. Samples of 20 μg of total RNA were denatured, separated by electrophoresis in a 1% agarose gel containing formaldehyde, and transferred to GeneScreen membranes (NEN, DuPont, MA). The membranes were prehybridized and then hybridized with p300 cDNA probes donated by Antonio Giordano labeled with [α-^{32}P] deoxy cytidine triphosphate using a random primer labeling system (Amersham Pharmacia Biotech, Buckinghamshire, UK). After hybridization, the membranes were washed and exposed to x-ray film. All blots were rehybridized with a glyceraldehyde-3-phosphate dehydrogenase (GAPDH) cDNA probe to normalize for mRNA loading differences. For the contents of mRNA to be quantified in the cells, the membranes were exposed to imaging plates, and radioactivities were measured with a bioimage analyzer (Fijix BAS 1500, Fuji Film, Tokyo).

Results

Tissue Patterns of p300 and CBP HAT Activities

Table 1 shows the HAT activity patterns of p300 and CBP in different tissues of normal young and old mice, respectively. Although the HAT activities of CBP were

Table 1. HAT Activity Assay of p300 and CBP in Different Tissues of Young and Old Mice

	p300			CBP		
Tissue	3 mo	24 mo	Statistics	3 mo	24 mo	Statistics
Kidney	Undetectable*	Undetectable*	—	1573 ± 290†	1758 ± 278†	NS
Heart	6090 ± 850†	6556 ± 756†	NS	7334 ± 666	7659 ± 999†	NS
Liver*	1365 ± 689*	733 ± 380*	$p < .01$	3192 ± 454*	1938 ± 227*	$p < .01$
Brain	9433 ± 964*	9803 ±1010*	NS	10522 ± 1465*	10695 ± 1725*	NS
Muscle	3380 ± 978*	2198 ± 366*	$p < .05$	4678 ± 1428*	3219 ± 783*	$p < .05$
Lung	7308 ± 950†	8446 ± 899†	NS	8993 ± 967†	9031 ± 952†	NS
Spleen	6857 ± 1546*	6767 ± 1039*	NS	8656 ± 1701†	9031 ± 2415†	NS
Testes	4686 ± 1217*	3243 ± 830*	$p < .01$	6579 ± 1439*	5005 ± 1174*	$p < .05$

Notes: Values are subtracted from normal IgG controls; they are mean ± 1 standard error. Student's *t* test was used. CBP = CREB-binding protein (CREB = cyclic adenosine monophosphate-regulated enhancer-biding protein); p300 = homologue protein; NS = not significant; HAT = histone acetyltransferase.

*Value is $n = 6$. †Value is $n = 4$.

slightly higher than that of p300, the tissue patterns of HAT activities of CBP and p300 were quite similar. The highest HAT activities were observed in the brain in both young and old mice. The lung, spleen, and heart had relatively high HAT activities. The testes and the muscle had intermediate HAT activities and the liver had low HAT activities. Among the tissues examined, the kidney showed the lowest HAT activities of p300 and CBP. These results revealed the tissue-specific patterns of the HAT activities of p300 and CBP in normal murine tissues and the similar enzymatic distribution of p300 and CBP in murine tissues.

To ensure the specificity of p300 and CBP in our HAT assay, we designed our experimental protocols especially at three points. First, we used a highly stringent Lysis buffer for cell lyzing and immunoprecipitation, because the deoxycholate and SDS contained in this buffer will diminish most, if not all, of the nonspecific protein interaction. Second, the data were subtracted from nonspecific IgG controls for every sample. The measuring values of specific HAT activity were always higher than 1000-fold of normal IgG controls. The data shown in Table 1 were the specific values subtracted from the control value. Third, we selectively used the antibodies without cross-reaction between p300 and CBP for immunoprecipitation, according to the information of the manufacturers (Santa Cruz). In fact, we confirmed the specificities of both the anti-p300 antibody and anti-CBP antibody we used for immunoprecipitation by Western blotting (data not shown).

Tissue Patterns of Total Cellular HAT Activities

To further understand the contribution of p300–CBP HAT activities in different tissues, we assayed the total cellular HAT activity by using total cell lysate. The results are shown in Table 2. When comparing Table 1 with Table 2, we found that the total cellular HAT activities not only had their own tissue patterns, which were significantly distinct from the tissue paterns of CBP and p300 HAT activities, but also showed even greater tissue diversity. The spleen and lung had the highest total cellular HAT activities; the heart, brain, muscle, and liver showed modest total cellular HAT activities; the kidney had very low total mixed HAT activities; and the total cellular HAT activities of the testes were undetectable. Taken together, these results suggested that, as did p300–CBP HAT activities, the total cellular HAT activities had their own distinct tissue patterns also.

Effect of Aging on HAT Activity of p300 and CBP

Table 1 also shows that there were no significant changes of p300 and CBP HAT activities with advancing age in most tissues examined, such as kidney, heart, brain, lung, and spleen. However, the HAT activities of both CBP and p300 in liver, muscle, and testes were significantly decreased with advancing age. Aging also had an effect on total cellular HAT activities. Table 2 shows that the total HAT activity of the spleen was significantly elevated in the 24-month-old group, whereas in other tissues no age-related changes of the total HAT activities were observed. These results indicated that there were age-related changes of p300–CBP HAT activities in liver, muscle, and testes, and there were changes of total cellular HAT activities in the spleen. However, in other tissues examined, the HAT activities of p300 and CBP and the total HAT activities were kept relatively stable in advancing age.

Effect of Development on HAT Activities of CBP and p300 in Brain and Liver

To understand if CBP and p300 HAT activities are associated with development, we further examined p300 and CBP HAT activities of liver and brain in fetal (E14), newborn (1 day) and 1-month-old mice. The results are shown in Table 3. The p300 and CBP HAT activities of liver and brain in fetal and newborn mice were much higher than those of other age groups, and those were downregulated with development. The most significant changes of HAT activities in the brain were observed between newborn and 1-month-old mice, whereas in liver, the decrease of HAT activities was more obvious between fetal and newborn mice than between newborn and 1-month-old mice. These results suggest that the HAT activities of p300 and CBP may play an important role in the development of brain and liver.

The mRNA Expression of p300 in Liver at Different Ages

In order to further clarify the great changes of p300 (CBP) HAT activities in liver, we examined the p300 mRNA expression of liver tissues from fetal (E14) to aged (24-month-old) mice. The p300 mRNA of E14 fetal mice was much higher than that of 1-month-old mice. The level of p300 mRNA gradually decreased with advancing age (Figure 1), although the levels of p300 mRNA of other tis-

Table 2. Total HAT Activity Assay in Different Tissues of Young and Old Mice

Tissue	3-mo	*n*	24-mo	*n*	Statistics
Kidney	2136 ± 756	5	2651 ± 801	5	NS
Heart	7354 ± 3607	5	8308 ± 3674	5	NS
Liver	5065 ± 1450	5	5969 ± 1892	5	NS
Brain	11618 ± 2953	7	10570 ± 3080	7	NS
Muscle	6532 ± 2158	8	5550 ± 1549	7	NS
Lung	27120 ± 1646	7	31066 ± 2360	7	NS
Spleen	29762 ± 6075	9	45122 ± 4835	10	$p < .01$
Testes	Undetectable	5	Undetectable	5	—

Notes: Values are mean ± 1 standard error. Student's *t* test was used. HAT = histone acetyltransferase; NS = not significant.

Table 3. Changes of p300 and CBP Activities in Liver and Brain With Development

	Liver		Brain	
Age	p300	CBP	p300	CBP
Fetus	11236 ± 1501	12832 ± 1452	15639 ± 1501	19740 ± 1954
Newborn	5958 ± 1275	8882 ± 1125	14537 ± 670	18535 ± 1076
1 mo	2478 ± 447	5308 ± 2343	10995 ± 776	13355 ± 2736
3 mo	1365 ± 689	3192 ± 454	9433 ± 964	10522 ± 1465
24 mo	733 ± 380	1810 ± 191	9803 ± 1010	10695 ± 1725

Notes: Values are subtracted from normal IgG controls; they are mean ± 1 standard error. CBP = CREB-binding protein (CREB = cyclic adenosine monophosphate-regulated enhancer-binding protein); p300 = homologue protein.

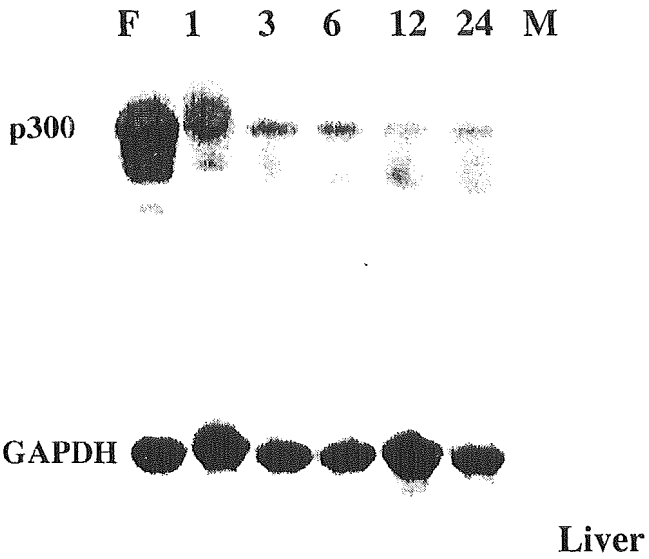

Figure 1. The expression of p300 mRNA in murine liver: 20 μg of total RNA was subjected to Northern blot analysis probed with segment of p300 cDNA, which was followed by a glyceraldehyde-3-phosphate dehydrogenase (GAPDH) probe to normalize for loading differences. F = 14-day-old murine fetus; M = month.

sues were relatively stable in advancing age (data not shown).

Discussion

Tissue Patterns of p300 and CBP HAT Activities

Although p300 and CBP have been reported to be ubiquitously expressed in cell lines derived from different tissues, we presented here that HAT activities of both p300 and CBP have distinct tissue patterns (Tables 1 and 2). This distinct tissue pattern of HAT activities suggests that, before functioning as the important coactivators of gene transcription, p300 and CBP are regulated by the still unknown mechanism(s) for their own HAT activities. We found significant differences in tissue patterns between p300 and CBP HAT activities and total cellular HAT activities. The highest HAT activity of p300 and CBP versus relatively low total cellular HAT activities in the brain indicated that p300 and CBP might play important roles for gene transcription in the brain. In contrast, the very high total cellular HAT activities over the HAT activities of p300 and CBP in the spleen and lung might mean that the HAT other than p300–CBP activities were also important in transcriptional regulation. One extreme example we found was in the testes. Testes showed high HAT activities of p300 and CBP, but the total cellular HAT activities were undetectable. Given that we used more than 60-fold of cell lysates (1 mg) for p300–CBP immunoprecipitation and their specific HAT assay than those (15 μg) for total cellular HAT assay, the higher HAT activities of p300–CBP than total cellular HAT activities is not unreasonable. However, in comparison with other tissues with similar p300–CBP HAT activities, such as the heart, the total cellular HAT activities in testes were really very weak. Therefore, we hypothesize here that the p300 and CBP might be the main HAT in testes, and their activities might be essential in testis development and spermatogenesis. Further studies should be carried out to investigate the tissue patterns of other HATs, such as p300/cyclic AMP responsible element binding protein-associated factor (25), general control nonrepressed 5, and so on.

Effect of Aging on HAT Activity of p300 and CBP

There have been no reports about the effect of aging on HAT activities of CBP and p300. The data presented herein showed that in most examined tissues, such as the kidney, brain, heart, lung, and spleen, HAT activities of p300 and CBP are considerably stable with advancing age, indicating that HAT activities of p300 and CBP are associated with the transcription activation–regulation of genes responsible for the physiological changes of aging. However, in liver, muscle and testes, HAT activities of p300 and CBP were attenuated with aging, although the underlying mechanisms are unclear. It is interesting to find that the total cellular HAT activity in spleen of 24-month-old mice is obviously elevated whereas the HAT activities of p300 and CBP are kept unchanged with advancing age. The spleen is an immune organ and there are reports that demonstrate the changes of T-cell subpopulations and related cytokine production of the spleen with aging (26,27). We suppose, therefore, that the increased total cellular HAT activities in spleen of old mice are concerned with these changes and HATs other than p300 and CBP may be involved. The changes of HAT activities in the spleen of old mice might be due to an increased sensitivity of the old mice to infection. However, this possibility is negligible, because our animal center is a strictly pathogen-free environment. In brief, our results support that HAT activities of p300 and CBP are differently changed in normal murine tissues with advancing age, and further studies are needed for elucidating the mechanism for regulation of p300 and CBP HAT activity in liver, muscle, and testes.

The Changes of p300 and CBP HAT Activities With Development

The important functions of p300 and CBP in development have been proved by gene targeting. The homozygous CBP-deficient mice died around E10.5–E12.5, apparently as a result of massive hemorrhage caused by defective blood vessel formation in the central nervous system, and they exhibited apparent development retardation as well as delays in both primitive and definitive hematopoiesis (28). CBP-deficient murine embryos also exhibited defective neural tube closure (28). Similar to the exhibitions of the CBP-deficient mice, the mice lacking a functional p300 gene died between days 9 and 11.5 of gestation, exhibiting defects in neurulation, cell proliferation, and heart development (29). Cells derived from p300-deficient embryos also displayed specific transcriptional defects and poor proliferation (29). Our data showing much higher HAT activities of p300 and CBP in brains of the E14 fetus and newborns than in those of other age groups, and the markedly downregulated HAT activities of p300 and CBP with the development of the brain (Table 3) were consistent with the reports stated above. Our results indicate that HAT activities of p300 and

CBP play an important role in the development of brain. Furthermore, our findings that very high HAT activities of p300 and CBP were observed in liver of 14-day gestational fetuses and that they subsequently sharply declined with liver development appears to support the notion that HAT activities of p300 and CBP are associated with the hematopoiesis of fetal liver. Liver is one of the main hematopoietic tissues of the fetus during gestation. Murine hepatic hematopoiesis started at 11 days gestation (30), and different types of Spleen-colony-forming units attained peaks at 13–14 days gestation (31); after that, the hepatic hematopoiesis quickly decreased with development. The changes of p300 and CBP HAT activities in liver were in accordance with reports that CBP-deficient mice exhibited delays in both primitive and definitive hematopoiesis and appear to suggest that HAT activities of p300 and CBP are responsible for fetal liver hematopoiesis.

Taken together, HAT activities of p300 and CBP have distinct tissue patterns and maintain considerable stability with advancing age in most murine tissues except liver, muscle, and testes. The alteration of p300–CBP activation might be associated with the development of brain and fetal hepatic hematopoiesis.

Histone Acetylation in Aging

Ogryzko and colleagues (32) showed that two histone deacetylase inhibitors, sodium butyrate and trichostatin A, dramatically reduced the human diploid fibroblast proliferative life span. We have shown that histone deacetylase inhibitor (sodium butyrate or trichostatin A) induces a cellular senescence-like phenotype in NIH3T3 cells and enhances p21 promoter activity in this cell line (33). We also found that p300 works as a coactivator of trichostatin A-induced p21 promoter activity (34). Meanwhile, Wagner and colleagues (35) found a significant decrease in the abundance of histone deacetylase-1 in senescent cells by Northern blot and Western blot analyses. These results strongly suggest that, on one hand, histone acetylation may play some role in cellular senescence. On the other hand, to our knowledge there have been no reports that have proven the role of histone acetylation in the in vivo aging of mammals. To our knowledge, the data presented here are the first report concerned with this issue. We think they will be useful in the development of our understanding of the role of histone acetylation in the in vivo aging process from the view of gene transcription.

ACKNOWLEDGMENTS

This work was supported by the Fund for Comprehensive Research on Aging and Health.

Address correspondence to Dr. Ken-ichi Isobe, Department of Basic Gerontology, National Institute for Longevity Sciences, 36-3, Gengo, Morioka-cho, Obu, Aichi, 474-8522, Japan. E-mail: kenisobe@nils.go.jp

REFERENCES

1. Chriviaq JC, Kwok RP, Lamb N, Hagiwara M, Montminy MR, Goodman R. Phosphorylated CREB binds specifically to the nuclear protein CBP. *Nature.* 1993;365(6449):855–859.
2. Andrisani OM. CREB-mediated transcription control. *Crit Rev Eukaryot Gene Expr.* 1999;9(1):19–32.
3. Eckner R, Ewen ME, Newsome D, et al. Molecular cloning and functional analysis of the adenovirus E1A-associated 300-kDa protein (p300) reveals a protein with properties of a transcriptional adapter. *Genes Dev.* 1994;8:869–884.
4. Arany Z, Newsome D, Oldread E, Livingston DM, Eckner R. A family of transcriptional adaptor proteins targeted by the E1A oncoprotein. *Nature.* 1995;374:81–84.
5. Lundblad JR, Kwok RPS, Laurance ME, Harter ML, Goodman RH. Adenoviral E1A-associated protein p300 as a functional homologue of the transcriptional co-activator CBP. *Nature.* 1995;374:85–88.
6. Egan C, Jelsma TN, Howe JA, Bayley ST, Ferguson B, Branton PE. Mapping of cellular protein-binding sites on the products of early-region 1A of human adenovirus type 5. *Mol Cell Biol.* 1988;8:3955–3959.
7. Whyte P, Williamson NM, Harlow E. Cellular targets for transformation by the adenovirus E1A proteins. *Cell.* 1989;56:67–75.
8. Yaciuk P, Moran E. Analysis with specific polyclonal antiserum indicates that the E1A-associated 300 kDa product is a stable nuclear phosphoprotein that undergoes cell cycle phase-specific modification. *Mol Cell Biol.* 1991;11(11):5389–5397.
9. Giles RH, Peters DJM, Breuning MH. Conjunction dysfunction: CBP/p300 in human disease. *Trends Genet.* 1998;14:178–183.
10. Janknecht R, Hunter TA. A growing coactivator network. *Nature.* 1996;383:22–23.
11. Ogryzko VV, Schiltz RL, Russanova V, Howard BH, Nakatani Y. The transcriptional coactivators p300 and CBP are histone acetyltransferases. *Cell.* 1996;87:953–959.
12. Andrew J, Kouzarides T. The CBP co-activator is a histone acetyltransferase. *Nature.* 1996;384:631–643.
13. Ait-Si-Ali S, Ramirez S, Barre F-X, et al. Histone acetyltransferase activity of CBP is controlled by cycle-dependent kinases and oncoprotein E1A. *Nature.* 1998;396:184–186.
14. Grunstein M. Histone acetylation in chromatin structure and transcription. *Nature.* 1997;389:349–352.
15. Mizzen CA, Allis CD. Linking histone acetylation to transcription regulation. *Cell Mol Life Sci.* 1998;54:6–20.
16. Struhl K. Histone acetylation and transcriptional regulatory mechanism. *Genes Dev.* 1998;12:599–606.
17. Kornberg RD, Lorch Y. Twenty-five years of the nucleosome, fundamental particle of the eukaryote chromosome. *Cell.* 1999;98:285–294.
18. Imhof A, Yang XJ, Ogryzko VV, Nakatani Y, Wolff AP, Ge H. Acetylation of general transcription factors by histone acetyltransferase. *Curr Biol.* 1997;7:689–692.
19. Ugai H, Uchida K, Kawasaki H, Yokoyama KK. The coactivator p300 and CBP have different functions during the differentiation of F9 cells. *J Mol Med.* 1999;77:481–494.
20. Gu W, Shi X, Roeder RG. Synergistic activation of transcription by CBP and p53. *Nature.* 1997;387:819–823.
21. Zhang W, Bieker JJ. Acetylation and modulation of erythroid Kruppel-like factor (EKLF) activity by interaction with histone acetyltransferases. *Proc Natl Acad Sci USA.* 1998;95:9855–9860.
22. Boyes J, Byfield P, Nakatani Y, Ogryzko V. Regulation of activity of the transcription factor GATA-1 by acetylation. *Nature.* 1998;396:594–598.
23. Perissi V, Dasen JS, Kurokawa R, et al. Factor-specific modulation of CREB-binding protein acetyltransferase activity. *Proc Natl Acad Sci USA.* 1999;96:3652–3657.
24. Yang XJ, Ogryzko VV, Nishikawa J, Howard BH, Nakatani Y. A p300/CBP-associated factor that competes with the adenoviral oncoprotein E1A. *Nature.* 1996;382:319–324.
25. Xu W, Edmondson DG, Roth JY. Mammalian GCNS and P/CAF acetyltransferases have homologous amino-terminal domains important for recognition of nucleosomal substrates. *Mol Cell Biol.* 1998;18:5659–5669.
26. Takayama E, Seki S, Ohkawa T, et al. Mouse CD8÷ CD122+ T cells with intermediate TCR increasing with age provide a source of early IFN-gamma production. *J Immunol.* 2000;164:5652–5658.
27. Wakikawa A, Utsuyama M, Wakabayashi A, Kitagawa M, Hirokawa K. Age-related alteration of cytokine production profile by T cell subsets in mice: a flow cytometric study. *Exp Gerontol.* 1999;34:231–242.
28. Tanaka Y, Naruse I, Hong T, et al. Extensive brain hemorrhage and embryonic lethality in a mouse null mutant of CREB-binding protein. *Mech Dev.* 2000;95:133–145.

29. Yao TP, Oh SP, Fuchs M, et al. Gene dosage-dependent embryonic development and proliferation defects in mice lacking the transcriptional integrator p300. *Cell.* 1998;93:361–372.
30. Sasaki K, Matsumura G. Hemopoietic cells in the liver and spleen of the embryonic and early postnatal mouse: a karyometrical observation. *Anat Rec.* 1987;219:378–383.
31. Corso A, Hogeweg-Platenburg MG, De Vries P, Visser JW. A protocol for the enrichment of different types of CFU-S from fetal mouse liver. *Hematologica.* 1993;78:5–11.
32. Ogryzko VV, Hirai TH, Russanova VR, Barbie DA, Howard BH. Human fibroblast commitment to a senescence-like state in response to histone deacetylase inhibitors is cell cycle dependent. *Mol Cell Biol.* 1996;16:5210–5218.
33. Xiao H, Hasegawa T, Miyaishi O, Ohkusu K, Isobe K. Sodium butyrate induces NIH3T3 cells to senescence-like state and enhances promoter activity of p21WAF/CIP1 in p53-independent manner. *Biochem Biophys Res Commun.* 1997;237:457–460.
34. Xiao H, Hasegawa T, Isobe K. p300 collaborates with Sp1 and Sp3 in p21(waf1/cip1) promoter activation induced by histone deacetylase inhibitor. *J Biol Chem.* 2000;275:1371–1376.
35. Wagner M, Brosch G, Zwerschke W, Seto E, Loidl P, Jansen-Durr P. Histone deacetylases in replicative senescence: evidence for a senescence-specific form of HDAC-2. *FEBS Lett.* 2001;499:101–106.

Received May 22, 2001
Accepted October 25, 2001
Decision Editor: John A. Faulkner, PhD

Journal of Cellular Biochemistry 84:401–407 (2002)

Genomic Cloning and Promoter Analysis of the *GAHSP40* Gene

Fumiyasu Hamajima,[1,2] Tadao Hasegawa,[1] Izumi Nakashima,[2] and Ken-ichi Isobe[1]*

[1]Department of Basic Gerontology, National Institute for Longevity Sciences, 36-3 Gengo Morioka-Cho Obu, Aichi 474-8522 Japan

[2]Department of Immunology, Nagoya University, Graduate School of Medicine, Turumai-Cho-Showa-Ku, Nagoya, Japan

Abstract The new heat shock protein (GAHSP40), which binds to Gadd34, is a member of the Hsp40 family gene and has a J domain, which is similar to bacterial DNAJ. We have isolated and sequenced the mouse *GAHSP40* gene including 1.6 kb of the 5′-flanking region. Primer extension analysis revealed that the transcription initiation site was located 36-bp upstream of the ATG translation initiation codon. In order to identify the heat-responsive regions in the *GAHSP40*, NIH3T3 cells were transiently transfected with a series of 5′ terminus-truncated mutants of the *GAHSP40* promoter linked to the luciferase reporter gene. We found that the region of −284 to −184 bp from initiation start site responded to heat shock treatment. By the gel shift analysis, we found the heat shock elements (HSEs) located in this region from −257 to −225. This HSEs has five 5 bp motifs. The transfection studies using HSEs mutant vectors revealed that those 3′ two 5 bp motifs are essential for heat responsive transcription. J. Cell. Biochem. 84: 401–407, 2002.

Key words: GADD34; heat shock factor; heat shock element

Cells, subjected to stress, respond by synthesizing a group of evolutionarily conserved proteins called heat shock proteins (HSPs). These stress-induced proteins perform many essential roles in cell survival, including prevention of protein aggregation and facilitation of protein folding. HSP40 family is one of the HSPs containing the DNAJ homologous region of *Escherichia coli*, J-domain of DNAJ. The main future of DNAJ function is the ability to directly interact with DNAK to stimulate ATPase activity and act as a chaperon in conjunction with DNAK [Georgopoulos, 1992]. DNAJ like HSP40 proteins have been isolated in yeast (SEC63/NPL1, SCJ1, YDJ1, SIS1, Zuotin), plant (ANJ1), fruit fly (Csp29, Csp32), mammalian (Csp1, Csp2, MTJ1, and ZRF1), and human cells (HDJ-1, HDJ2, HSJ1, HSDJ, HSPF1, and HLJ1) [Sadler et al., 1989; Ohtsuka et al., 1990; Zinsmaier et al., 1990; Blumberg and Silver, 1991; Caplan and Douglas, 1991; Luke et al., 1991; Atencio and Yaffe, 1992; Zhang et al., 1992; Zhu et al., 1993; Brightman et al., 1995; Hughes et al., 1995; Chamberlain and Burgoyne, 1996; Hoe et al., 1998], and their functions are under investigation [Raabe and Manley, 1991; Cheetham et al., 1992; Chellaiah et al, 1993; Oh et al., 1993; Ohtsuka, 1993; Hata et al., 1996; Kelley, 1998].

Previously, in order to examine the function of GADD34, we used the yeast two-hybrid system to clone the protein that interacts with the murine GADD34. We have cloned new HSP40 family gene, *GAHSP40* [Hasegawa et al., 2000]. *GAHSP40* is about a 1.4-kb gene and the N-terminal 70 amino acids correspond to the J-domain, which has been demonstrated to be the HSP70 interaction region and conserved among all proteins defined as DNAJ family. GAHSP40 was induced not only by heat shock but also by MMS (methyl methanesulfonate), that is a DNA alkylating agent. One of the hallmarks of heat shock genes is the presence of

Grant sponsor: Fund for Comprehensive Research on Aging and Health, Ministry of Health and Welfare of Japan and in part Grant-in-Aid for Scientific research.

*Correspondence to: Ken-ichi Isobe, Department of Basic Gerontology, National Institute for Longevity Sciences, 36-3 Gengo Morioka-Cho Obu, Aichi 474-8522 Japan.
E-mail: kenisobe@nils.go.jp

Received 15 June 2001; Accepted 5 September 2001

Published online November 13, 2001.
DOI 10.1002/jcb.10029

heat shock elements (HSEs) in their 5′-flanking regions to which heat shock transcription factor (HSF) binds stimulating transcription. HSE has been defined as an array of adjacent inverted pentamers with the sequence 5′-nGAAn-3′ [Amin et al., 1988; Xiao and Lis, 1988]. HSE sequences in Human HSP40 gene were composed of eight contiguous nGAAn motifs and were essential for heat shock response. In this paper, we clone the 5′ flanking region of *GAHSP40* gene and examine the regulation of its expression responded to heat shock. We show that GAHSP40 also has HSE element, which is essential for heat shock response.

MATERIALS AND METHODS

Oligonucleotides

To determine the nucleotide sequence of clones, the following oligonucleotides were used: *Bca*BEST Sequencing Primer RV-M5′-GAGCGGATAACAATTTCACACAGG-3′, *Bca*BEST Sequencing Primer M13-47 5′-CGCCAGGGTTTTCCCAGTCACGAC-3′. To determine the transcription initiation site, the following oligonucleotides were used in primer extension experiments: 5′-CTGTAGCTCCTTTGTCAATTCCCA-3′.

Cell Culture

NIH3T3 cells from the American Type Culture Collection (ATCC, Rockville, MD) were maintained in a 37°C humidified atmosphere containing 5% CO_2 with Dulbecco's modified Eagle's medium (DMEM) supplemented with 10% fetal bovine serum (FBS).

Cloning and DNA Sequencing of Genomic DNA for GAHSP40

Screening of the Lambda FIX II library (Stratagene) isolated genomic clones with the mouse *GAHSP40* cDNA probe under high-stringency hybridization conditions.

Two isolated clones were cloned into pUC18 vector. The nucleotide sequence of each clone was determined by the ABI 377 autosequencer with *Bca*BEST Sequencing Primer RV-M and *Bca*BEST Sequencing Primer M13-47 (Takara). If necessary, oligonucleotides were chemically synthesized and were used as sequencing primers.

Primer Extension

Total cellular RNA was extracted from NIH3T3 cells at 42°C for 1 h by the method described elsewhere. A 25-mer primer, which was complementary to the region downstream of the ATG codon, was chemically synthesized. The 5′ end of the primer was labeled with [γ-^{32}P] and hybridized with 50 μg of total RNA for 16 h at 45°C in solution containing 80% formamide, 40 mM PIPES (pH 6.4), 1 mM EDTA, and 0.4 M NaCl. The RNA and primer were ethanol-precipitated and re-dissolved in a solution for primer extension. The primer was extended for 1 h at 42°C in a 9 μl reaction mixture containing 50 mM Tris-HCl, 50 mM KCl, 10 mM MgCl, 10 mM dithiothreitol, 1 mM each dNTP, 0.5 mM sperimidine, 6.2 mM sodium pyrophosphate, and 300 U AMV reverse transcriptase. After incubation, the reaction was stopped by adding 1 μl of 0.5 M EDTA, and 1 μl of RNase A (1 mg/ml) was added to digest RNA. The digestion was carried out for 30 min at 37°C. The reaction product was ethanol-precipitated and redissolved in 4 μl of Loading dye containing 98% formamide, 10mM EDTA, 0.1% xylene cyanol, and 0.1% bromophenol blue. The samples were analyzed by a gel electrophoresis under denaturing conditions, followed by autoradiography. The nucleotide positions were cumulatively determined with references to a sequencing reaction in which the same primer was used (Primer Extension System-AMV Reverse Transcriptase, Promega, Madison WI).

Plasmid Construction

GAHSP40 promoter-containing reporter constructs were made as follows: The phage positive clone was cut by EcoRI and subjected to southern hybridization. The 1.6 kb of EcoRI digested band was positively stained by GAHSP cDNA probe. This fragment was inserted into pUC18 EcoRI site. Then this construct was re-inserted into pGL3-basic luciferase vector (pGL3b-1557). The 5′-deletion mutants were obtained by making deletions in pGL3b-1557 by using an exonuclease III based system (Nippon Gene, deletion kit). To create a panel of site-directed mutants, mutagenesis of pGL3b-284 was performed using the QuikChange™ Site-Directed Mutagenesis Kit (Stratagene). The oligonucleotides used in these mutagenesis reactions are as follows: pGL3b-m1, 5′-GTTCGCTGTTAACTAAAGTACAGAG-3′ and 5′-TCTGTACTTTAGTTAACAGCGAA-3′; pGL3b-m2, 5′-GTAGCGTTCGTTAACTCGCTGTTCTAG-3′ and 5′-TAGAACAGCGAGTTAACGAACGCTA-3′; pGL3b-m3 5′-GTCCTGTAGCGTTA-

ACTCGTTCGCTG-3′ and 5′-AGCGAACGAGTTAACGCTACAGGA-3.

DNA Transfection and Luciferase Assay

NIH3T3 cells were plated onto 12-well plates at a density of 40,000 cells/plates. Cells were transfected with 2.5 μg/plates of plasmid by SuperFect Transfection Reagent (Qiagen, Hilden. Germany) according to the manufacturer's instructions. The test plasmid (2.25 μg/plates) and internal control plasmid (0.25 μg/plates) were co-transfected into cells. After 20 h incubation, the medium was replaced with fresh cell growth medium and the cells were grown for a further 20 h before heat shock treatment at 42°C for 6 h. The cells were harvested and lysed after heat shock treatment. The cell lysate was subjected to the assay for protein expression. The transfection efficiency was estimated via co-transfection with thimidine kinase promoter-driven *Renilla* luciferase reporter vector (pRL-TK plasmid, dual luciferase assay system, Promega, Madison, WI). The intensity of chemiluminescence was measured by a luminometer (Lumut LB9501, Berthold).

Gel Mobility Shift Assay

Nuclear extracts from either proliferating or heat shock treated NIH3T3 cells were prepared as described [Hasegawa et al., 1997]. A total of 5 μg of nuclear extract was incubated with 5 fmol of ^{32}P end labeled double-stranded oligonucleotides with a sequence corresponding to the region from −257 to −225 bp from initiation start site in the GAHSP40 promoter. Incubation was carried out in 1 volume of 10 μl at room temperature for 20 min. All binding reactions contained 10 mM Tris-HCl (pH 7.5), 4% glycerol, 50 mM NaCl, 0.5 mM EDTA, 0.5 mM dithiothreitol, 1 mM $MgCl_2$, and 0.5 mg/ml of poly (dI–dC). For competition, 1 pmol of unlabeled oligonucleotides was incubated in reactions. In supershift experiments, 1 μl of antibody was added 10 min before the labeled probe. The electrophoretic mobility shift assay products were separated on 4% polyacrylamide 0.5 × Tris-borate EDTA gel at room temperature at 150 V for 1.5 h. The gel was dried and subjected to autoradiography. The oligonucleotides used on these experiments were as follows: 5′-GTAGCGTTCGTTCGTTCGCTGTTCTAGAAAGTACAG-3′ and 5′-TGTACTTTCTAGAACAGCGAACGAACGAACGCTA-3′. The polyclonal antibodies used were from Santa Cruz Biotechnology (Santa Cruz, CA).

RESULTS

Cloning of the Gene for the GAHSP40

The 0.2-kb fragment that codes the regions of J domain was used as a probe to screen the mouse genomic library. Of approximately 1×10^6 clones screened, one positive clone was isolated. The complete nucleotide sequence of the region containing 1.6 kb genomic DNA was determined (Fig. 1).

Determination of Transcriptional Initiation Site of the *GAHSP40* Gene

The transcription initiation site of *GAHSP40* was determined by primer extension. Figure 2 shows the nucleotide sequence of the DNA near the 5′ end of *GAHSP40* mRNA. Alignment of nucleotides with genomic sequence indicated that the majority of transcription originates at or near c residue 36 nt upstream of the ATG initiation codon (Fig. 3). Typical TATA box was not present in the 1.6 kb region of the *GAHSP40* promoter.

Determination of the Promoter Region of the *GAHSP40* Gene

In order to identify the heat-responsive regions in the *GAHSP40*, NIH3T3 cells were transiently transfected with a series of 5′ terminus-truncated mutants of the *GAHSP40* promoter linked to the luciferase reporter gene. The transfected cells were either kept in DMEM medium or heat shocked (42°C, 6 h) before luciferase assay. As shown in Figure 4, heat shock induced more than a 25-fold expression compared to basal level in the cells transfected with the pGL3b-1557. Until the deletion to −284, all the constructs responded to heat shock (approximately 10–15-fold compared to basal level). The luciferase activity of pGL3b-184 was dramatically decreased in basal and heat shock state. These results showed that the region of −284 to −184 bp from the initiation start site responded to heat shock treatment.

Identification of the Nuclear Factors Involved in Heat Shock Response

In order to identify the proteins that bind to this region (from −284 to −184), Gel shift assay was performed with ^{32}P-labeled oligonucleotides and nuclear extracts from cultured

```
.-1557
TTCGAGCTTCATGTTAATAGAAGAATTCAATTTTTAAATGCAGTTAATTTACTAATTGTA
GTTTCTCTTCTCTTCATAGTCTCTCTCAAGTCTACCCCCTACACCTGTATTAGCAGGTAG
ATATTTATAGGTGAGTGTGATGGCATATGCACTTTCAGAGTCGCACTCTCATGATGACTG
CTGATGTTAACTTCCCCATGGTCTTTGGGACATGGAATGTGAAAAAGAAATGTTTGATCC

                                                    .-1266
TGATCCTTTCTCTGTGATAACTCCAGCTTGTGTCAAGTTGACACACAAAGCCAGCTGGTA
CAGATTGAAAACCCACAAAAGAGATAAAAGATGAGTTATTTACATTCAAAATATTTCTCA
TCTATTCAAGATACATTTTTAAAGAAGGAAAGCATCAGATAACATATAAATGTAAAATGA
TTAAAACTGTTGATTTAAAAAATTACAACAAATCGCAACAAATGTTTTTTAAAGGTATGA
AATATACTAATATTACAAGGGAATACTAAAAAGATAGGGAGAAAACCCCCCCCCACTTGT
TTCAAAAAAATCTTTGTCAACAAGTAAATACTTAAAATTAGGGGAAATGTGTTTTGAAGG

                .-933
AACTTGTTACCTAACTGCCTCTCCTAACTAATCCATCCAGGCCGTAAACTGGTCCCGGGT
GACAGTTACACTGACCTGAGCGTGCTGGAATCTGATCCTCTCTCCCCTACATTCCCTGCA
GTATAAAGACCCCCTCAGAATGGGCTTTTCCGTTTCATTGTGATAAGGAATGGTTTATTA

                                                .-734
AGTATTATCCCCCCTCCAAAAAAAAGAACCCCTAGTTAAAACCATTCTTAAGTCACCTAT
TTATGTTAAAATACTGCTTTTCAATGTTATAACAGTCCTTTTACCATGTGACATTTTATA

                .-634
TAGTGGCTCCCTCACTTTTCAGATCGATAGACCCCAGAAATTTTGAAAATGACCCAAATT
ATTTGAAGATTTTAAATGTAAACACCTCATATTTTAGTTCTGCACATTTTATAGCTAGGT

                                                .-488
AACCTTGAAATTGAAGTTAGAATACCTACTGTAAGTTGAGGGCTTTTCTGACTGTATAAT
CAGTTTAACATGGGATGCCTAATGGCTATAATTATTTCTGTTGCCTTTTTACCTCTAATG

                                .-384
GAGTAAATGTATATGTAGTTGCGGCATTCTGTGCTGGTTTGCTAAATCCACAGGAAATAA
AAGGGTACAGCTAGGACGAAGGAAAGGGAATAGTTAATCGTGGAGGAGGAGAGGCACAGC

            .-284
TCAGTACTTTGCCTAGAGGCCGCTGGGAAAGTGACGTCCTGTAGCGTTCGTTCGTTCGCT
                                                HSEs
                                                .-184
GTTCTAGAAAGTACAGAGACACGTAGTTGAAGTGGGAGGGTCTAGCTGAGGCCGTCTCCG

TGCGGTGTCTATTTATCTGTAAGTGAGCTGCCGGGGAGGAATTAAATAGAGACGCTGCCT
GCTGCCTCTGGACAGCTGAGCCGAGTTGCTGATTTGCTTTAACTTGTAAGATACCCAGCT

                                                +1
TGCTTTATTTTCTCAGGATCATTGTGTTGCTAAGCCTGGGGACGCTGTTTTCTTTTACAA

                                +37
AGGGAAATCTAAGTTCATTTCAAGGCATTCGAAATGGGGAAAGACTATTATCACATTTTG
                                M  G  K  D  Y  Y  H  I  L

GGAATTGACAAAGGAGCTACAGATGAAGATGTTAAAAAGGCTTACCGAAAGCAAGCCCTC
I  D  K  G  A  T  D  E  D  V  K  K  A  Y  R  K  Q  A  L  K

AAATTTCACCCGGACAAGAACAAATCTCCTCAAGCAGAGGAAAAATTTAAAGAGGTCGCA
F  H  P  D  K  N  K  S  P  Q  A  E  E  K  F  K  E  V  E  V  A  E

GAAGCGTATGAAGTACTGAGTGATCCTAAAAAGAGAGAAATATATGATCAGTTTGGCGAA
A  Y  E  V  L  S  D  P  K  K  R  E  I  Y  D  Q  F  G  E  E

gaaggtaagctgcatatttctgtacctttggcagtgtctgaatcgtagctttttttttttc
tctctctctcagccttctggttttt...
```

Fig. 1. Nucleotide sequence of the 5′ upstream region of the *GAHSP40* gene. Translation initiation codon (ATG) is indicated by the double underline. Arrowhead indicates the main transcription initiation site, which was denoted as +1. The intron sequences are indicated by lowercase letters. Dots indicate the deletion points of the constructs used in the reporter assay.

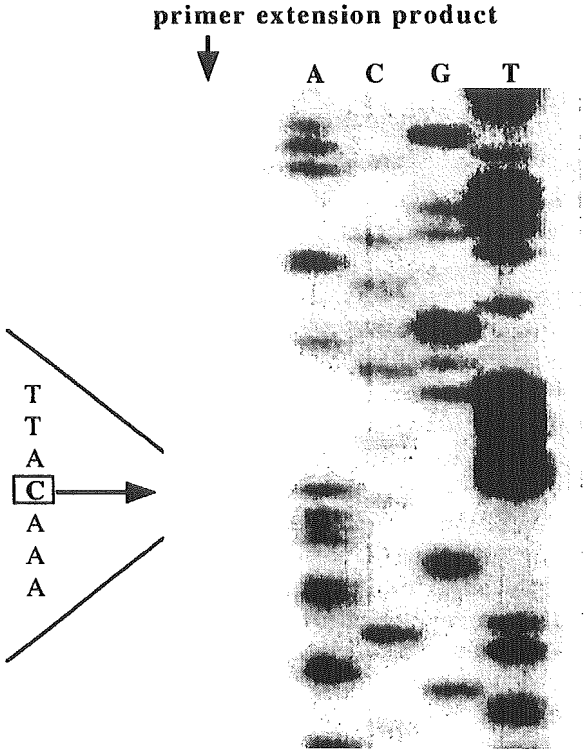

Fig. 2. Primer extension analysis of GAHSP40 mRNA. The major primer extension product is shown by an arrow. The DNA sequence of the GAHSP40 is shown on the left, and the nucleotide corresponding to the primer extension product is boxed.

NIH3T3 cells. (The probes used were −284 to −258, −257 to −225, and −224 to −185.) The positive bands were detected only by using the probe −257 to −225 (data not shown). According to database analysis, we noticed that there is a complex of HSEs (GTTCGTTCGTTCGCTG-TTCTAGAAA) in this region. We used −257 to −225 probe for Gel shift assay. Specific DNA–protein complexes were detected (Fig. 5). The specificity of these complexes was confirmed by competition, using excess amounts of unlabeled HSE-probe (lane 5), or with unrelated sequences (lane 6). The factors bound to HSE are

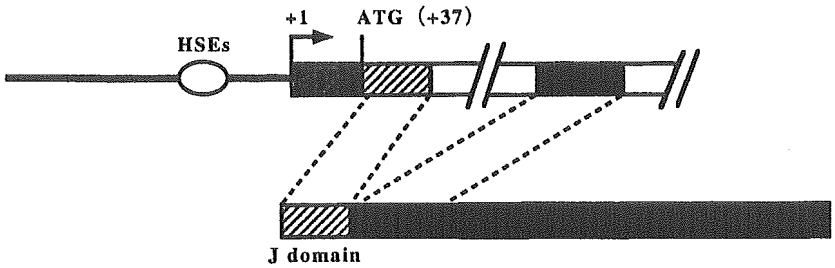

Fig. 3. Schematic structures of genomic and cDNA clones of GAHSP40. Filled boxes represent coding sequences. Open boxes represent noncoding sequences. Shaded boxes represent J domain motifs.

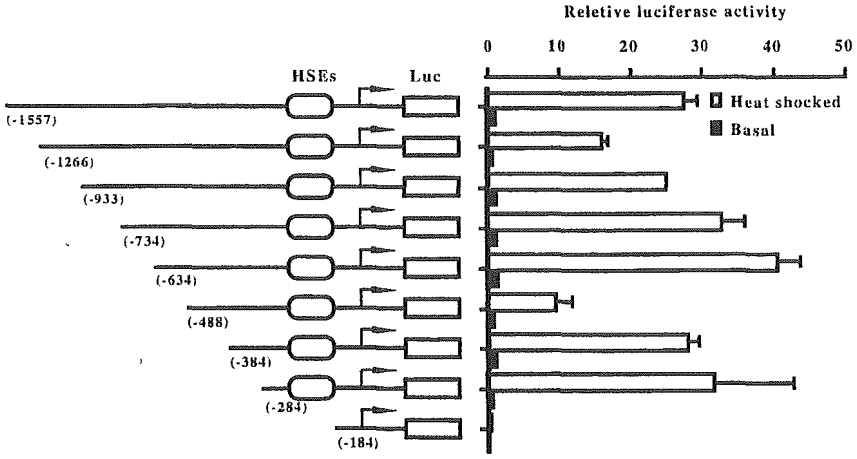

Fig. 4. Reporter assays on 5′ upstream region of *GAHSP40* gene. A 0.2 μg of wild type or 5′ terminus-truncated mutant *GAHSP40* promoter-firefly luciferase reporter constructs was transiently transfected into NIH3T3 cells. At 32 h after transfection, cells were either kept in DMEM medium or heat shocked (42°C, 6 h). Results were correlated with renilla luciferase activity that came from co-transfected pRL-TK and expressed as relative luciferase activity. The results are the mean and SD of six transfections from two separate experiments. The error bars indicate the SEM.

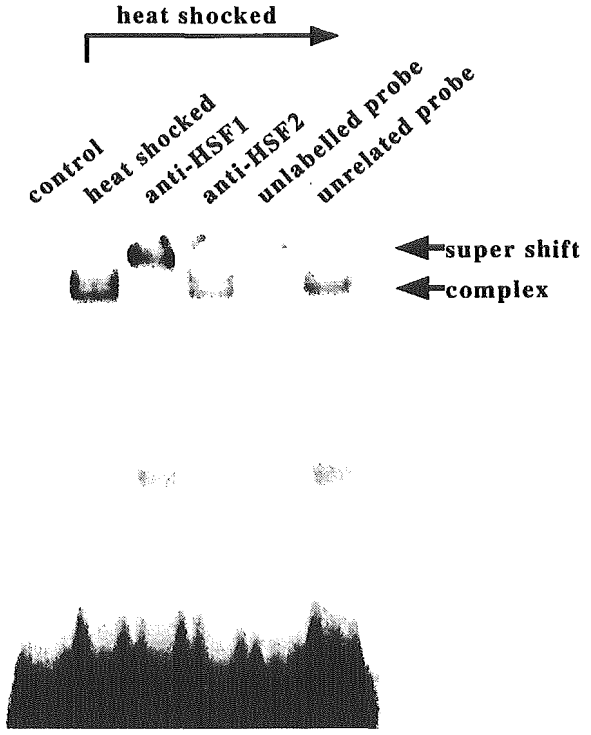

Fig. 5. Gel mobility assay. Nuclear extracts from NIH3T3 cells were incubated with ^{32}P-labeled HSE-probe correspond to −222 to −257 of wild-type GAHSP40 promoter sequence. **Lane 1**, extract from control cells; **lanes 2–6**, extract from heat shocked (42°C, 1 h) cells; pre-incubated with anti-HSF1 antibody; lane 4, pre-incubated with anti-HSF2 antibody; lane 5, 100-fold molar excess of unlabeled probe was added; lane 6, 100-fold molar excess of unrelated competitor (consensus SP1 binding sequence) was added.

known as HSF. To establish whether the DNA binding activity corresponds to HSF1, an antibody super-shift experiment was performed. As shown in Figure 5, supershifted band was detected only with the anti-HSF1 antibody (lane 3), not with anti-HSF2 antibody (lane 4). These results suggest that HSF is concerned with the expression of *GAHSP40* gene.

Effects of Mutations in HSE and Its Related Sequences on Promoter Activity of the *GAHSP40* Gene

To examine the role of these HSEs in *GAHSP40* promoter activity more precisely, site-directed mutations were introduced into the region from −284 to −184 bp of the *GAHSP40* promoter (Fig. 6). While other mutations did not significantly change the heat responsiveness, two mutations in HSE1 and HSE2 (pGL3-m2 in Fig. 6) decreased both basal and heat induced transcription. These results strongly suggest that the HSE1 and HSE2 located in the *GAHSP40* promoter are the *cis*-responsive elements for heat-induced transcription of *GAHSP40*.

DISCUSSION

We have cloned the 5′ region of the *GAHSP40* gene. Although several mammalians HSP40 cDNA have been reported, there exists no analysis of 5′ region of transcriptional regulation except human HSP40. Human HSP40 has TATA box, which lies 30 bp upstream of

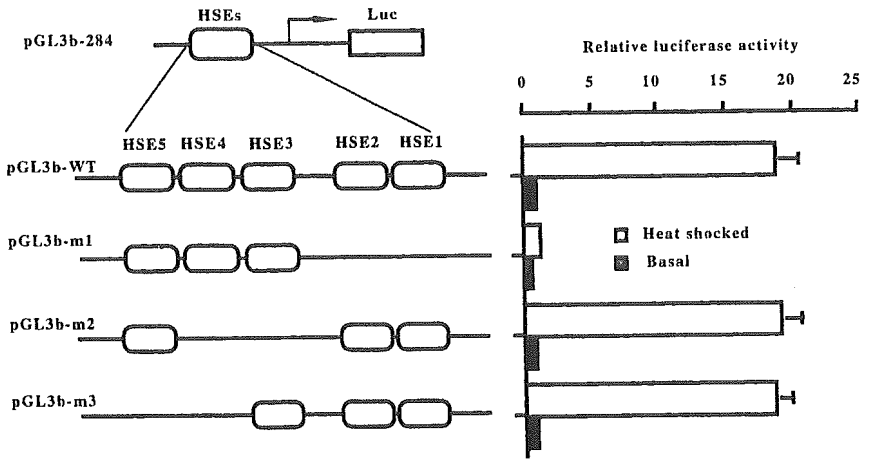

Fig. 6. Effects of mutations on promoter activity. A 0.2 μg of wild type or site-directed mutant *GAHSP40* −284 promoter constructs were transiently transfected into NIH3T3 cells. Transfected cells were kept in DMEM or heat shocked (42°C, 6 h). Luciferase activity was normalized and expressed as described in Figure 4. The results are the mean and SD of six separate transfections from two experiments. The SEM are indicated by error bar.

initiation start site. In contrast, *GAHSP40* has no TATA box. Human *HSP40* has GC-box and CAAT box, but *GAHSP40* has neither GC-box nor CAAT box.

Promoter analysis using deletion mutants defined that heat inducibility depends on the sequences from −284 to −184 position from major transcription start site. According to database analysis, we noticed that there are five 5-bp HSE motifs in this area. The protein factor bound to the HSE motifs is shown to be a HSF1 by gel mobility supershift analysis. In the case of human *HSP40*, GC-box and CAAT box had little effect to basal and heat inducible promoter activity. HSEs were both basic and heat inducible elements for human *HSP40*. This correlates to our *GAHSP40*. Both basal and heat inducible elements were laid in the HSEs. The difference between human *HSP40* and *GAHSP40* is that in human HSEs the first three 5 bp units are essential for promoter activity, whereas in *GAHSP40* last two 5 bp units are essential. HSEs in human *HSP40* is GGAAGGTTCTGGAGGGGGCTGGCGGGC-TCTGGAAGCTTCC. HSEs in *GAHSP40* is GTTCGTTCGTTCGCTGTTCTAGAAA. By introducing mutation to *HSP70* HSEs, it has been shown that possibly the trimeric structure of proteins bind to HSEs [Cunniff et al., 1991]. Heat shock elements are best described as contiguous arrays of variable numbers of the 5 bp-sequence nGAAn arranged in alternating orientation. At least two nGAAn units are needed for high affinity binding of heat shock factor in vitro [Sorger, 1991]. In our *GAHSP40* HSEs 3′ two 5 bp motifs are essential for transcription (Fig. 6). Taken together, these data show that different sequence HSEs in different promoters work as heat inducible *cis*-elements. In our *GAHSP40*, HSEs works not only as a heat-inducible *cis*-element but also works as a basal *cis*-element.

Although in many HSP promoter analyses such as human HSP40, HSP70 or HSP105, duration of heat shock treatments are 1 h (42°C), 6 h (42°C) are needed to induce *GAHSP40* promoter activity. This may come from the fact that the duration of mRNA expression of GAHSP40 is shorter than other HSPs [Hasegawa et al., 2000].

REFERENCES

Amin J, Ananthan J, Voellmy R. 1988. Key features of heat shock regulatory elements. Mol Cell Biol 8:3761–3769.

Atencio DP, Yaffe MP. 1992. MAS5, a yeast homolog of DNAJ involved in mitochondrial protein import. Mol Cell Biol 12:283–291.

Blumberg H, Silver PA. 1991. A homologue of the bacterial heat-shock gene DNAJ that alters protein sorting in yeast. Nature 349:627–630.

Brightman SE, Blatch GL, Zetter BR. 1995. Isolation of a mouse cDNA encoding MTJ1, a new murine member of the DNAJ family of proteins. Gene 153:249–254.

Caplan AJ, Douglas MG. 1991. Characterization of YDJ1: a yeast homologue of the bacterial DNAJ protein. J Cell Biol 114:609–621.

Chamberlain LH, Burgoyne RD. 1996. Identification of a novel cysteine string protein variant and expression of cysteine string proteins in non-neuronal cells. J Biol Chem 271:7320–7323.

Cheetham ME, Brion JP, Anderton BH. 1992. Human homologues of the bacterial heat-shock protein DNAJ are preferentially expressed in neurons. Biochem J 284:469–476.

Chellaiah A, Davis A, Mohanakumar T. 1993. Cloning of a unique human homologue of the *Escherichia coli* DNAJ heat shock protein. Biochim Biophys Acta 1174:111–113.

Cunniff NF, Wagner J, Morgan WD. 1991. Modular recognition of 5-base-pair DNA sequence motifs by human heat shock transcription factor. Mol Cell Biol 11:3504–3514.

Georgopoulos C. 1992. The emergence of the chaperone machines. Trends Biochem Sci 17:295–299.

Hasegawa T, Takeuchi A, Miyaishi O, Isobe K, de Crombrugghe B. 1997. Cloning and characterization of a transcription factor that binds to theproximal promoters of the two mouse type I collagen genes. J Biol Chem Feb 21:4915–4923.

Hasegawa T, Xiao H, Hamajima F, Isobe K. 2000. Interaction between DNA-damage protein GADD34 and a new member of the hsp40 family of heat shock proteins that is induced by a DNA-damaging reagent. Biochem J 352:795–800.

Hata M, Okumura K, Seto M, Ohtsuka K. 1996. Genomic cloning of a human heat shock protein 40 (Hsp40) gene (HSPF1) and its chromosomal localization to 19p13.2. Genomics 15:446–449.

Hoe KL, Won M, Chung KS, Jang YJ, Lee SB, Kim DU, Lee JW, Yun JH, Yoo HS. 1998. Isolation of a new member of DNAJ-like heat shock protein 40 (Hsp40) from human liver. Biochim Biophys Acta 1383:4–8.

Hughes R, Chan FY, White RA, Zon LI. 1995. Cloning and chromosomal localization of a mouse cDNA with homology to the *Saccharomyces cerevisiae* gene zuotin. Genomics 29:546–550.

Kelley WL. 1998. The J-domain family and the recruitment of chaperone power. Trends Biochem Sci 23:222–227.

Luke MM, Sutton A, Arndt KT. 1991. Characterization of SIS1, a *Saccharomyces cerevisiae* homologue of bacterial DNAJ proteins. J Cell Biol 114:623–638.

Oh S, Iwahori A, Kato S. 1993. Human cDNA encoding DNAJ protein homologue. Biochim Biophys Acta 1174:114–116.

Ohtsuka K. 1993. Cloning of a cDNA for heat-shock protein hsp40, a human homologue of bacterial DNAJ. Biochem Biophys Res Commun 197:235–240.

Ohtsuka K, Masuda A, Nakai A, Nagata K. 1990. A novel 40-kDa protein induced by heat shock and other stresses in mammalian and avian cells. Biochem Biophys Res Commun 166:642–647.

Raabe T, Manley JL. 1991. A human homologue of the *Escherichia coli* DNAJ heat-shock protein. Nucleic Acids Res 19:6645.

Sadler I, Chiang A, Kurihara T, Rothblatt J, Way J, Silver P. 1989. A yeast gene important for protein assembly into the endoplasmic reticulum and the nucleus has homology to DNAJ, an *Escherichia coli* heat shock protein. J Cell Biol 109:2665–2675.

Sorger PK. 1991. Heat shock factor and the heat shock response. Cell 65:363–366.

Xiao H, Lis JT. 1988. Germline transformation used to define key features of heat-shock response elements. Science 239:1139–1142.

Zhang S, Lockshin C, Herbert A, Winter E, Rich A. 1992. Zuotin, a putative Z-DNA binding protein in *Saccharomyces cerevisiae*. EMBO J 11:3787–3796.

Zhu JK, Shi J, Bressan RA, Hasegawa PM. 1993. Expression of an *Atriplex nummularia* gene encoding a protein homologous to the bacterial molecular chaperone DNAJ. Plant Cell 5:341–349.

Zinsmaier KE, Hofbauer A, Heimbeck G, Pflugfelder GO, Buchner S, Buchner E. 1990. A cysteine-string protein is expressed in retina and brain of *Drosophila*. J Neurogenet 7:15–29.

J Hepatobiliary Pancreat Surg (2002) 9:413–422

Journal of HBP Surgery

Evidence-based clinical practice guidelines for acute pancreatitis: proposals

Toshihiko Mayumi[1,*], Hideki Ura[2,*], Shinjyu Arata[3,*], Nobuya Kitamura[4,*], Ikuo Kiriyama[5,*], Kazuhiko Shibuya[6,*], Miho Sekimoto[7,*], Naoki Nago[8,*], Masahiko Hirota[9,*], Masahiko Yoshida[10,*], Yasuo Ito[11,*], Koichi Hirata[12,*], and Tadahiro Takada[10,**]

[1] Department of Emergency Medicine and Intensive Care, Nagoya University School of Medicine, 65 Tsurumai-cho, Showa-ku, Nagoya, Aichi 466-8560, Japan
[2] Department of Traumatology and Critical Care Medicine, Sapporo Medical University School of Medicine, Sapporo, Japan
[3] Critical Care Emergency Center, Yokohama City University School of Medicine, Yokohama, Japan
[4] Department of Emergency and Critical Care Medicine, Graduate School of Medicine, Chiba University, Chiba, Japan
[5] Department of Gastroenterology, Ogaki Municipal Hospital, Ogaki, Japan
[6] Division of Gastroenterological Surgery, Tohoku University Graduate School of Medicine, Sendai, Japan
[7] Department of General Medicine, Kyoto University School of Medicine, Kyoto, Japan
[8] Tsukude National Health Insurance Clinic, Minami-Shitara, Japan
[9] Second Department of Surgery, Kumamoto University Medical School, Kumamoto, Japan
[10] Department of Surgery, Teikyo University School of Medicine, Tokyo, Japan
[11] Department of Pediatric Surgery, Kyorin University School of Medicine, Mitaka, Tokyo, Japan
[12] First Department of Surgery, Sapporo Medical University School of Medicine, Sapporo, Japan

Abstract
Background/Purpose. To provide a framework for clinicians to manage acute pancreatitis, evidence-based guidelines have been developed by the Japanese Society of Abdominal Emergency Medicine.
Methods. Evidence was collected by a systematic search of MEDLINE and Japana Centra Revuo Medicina. A total of 1348 papers were reviewed and levels of evidence were assessed. Practical recommendations were also graded.
Results. The present guidelines consist of introductions, a summary of recommendations, practice algorithms, definitions, epidemiology, diagnosis, severity assessment, and therapy. The main points of recommendation in these guidelines are: (1) measuring lipase for the diagnosis of acute pancreatitis (recommendation grade [RG], A). (2) The Severity of acute pancreatitis should be assessed using a scoring system, such as that of the Japanese Ministry of Health and Welfare or Acute Physiology and Chronic Health Evaluation (APACHE) II (RG, A). (3) Enhanced computed tomography (CT) should be used for assessment of degree of pancreatic necrosis and inflammation (RG, B). (4) Prophylactic antibiotic administration should be used for severe pancreatitis (RG, A), but not for mild to moderate pancreatitis (RG, D). (5) Gabexate mesilate should be used for severe pancreatitis (RG, B). (6) Enteral feeding should be used for all pancreatitis (RG, B). (7) Continuous hemodiafiltration and continuous arterial infusion of proteinase inhibitor and antibiotics may be of benefit (RG, C). (8) Fine-needle aspiration should be done for the diagnosis of infectious pancreatic necrosis, and if positive, necrosectomy is indicated (RG, A).
Conclusions. These guidelines provide useful information for physicians to manage this troublesome disease.

Key words Evidence-based medicine · Acute pancreatitis · Guidelines · Recommendation · Scoring system

Offprint requests to: T. Mayumi
* Working Group for the Practical Guidelines for Acute Pancreatitis of the Japanese Society of Emergency Abdominal Medicine
** President of the Japanese Society of Emergency Abdominal Medicine, Tokyo, Japan
Received: May 6, 2002 / Accepted: May 17, 2002

Background and purpose of guidelines

There are several clinical guidelines and recommendations for acute pancreatitis.[1,2] During recent years many diagnostic and therapeutic methods have been developed for the disease. But some of these interventions for acute pancreatitis are used only in Japan, and not in other countries. In this situation, differences in interventions for the disease between institutions are increasing. However, despite these attempts to intervene in the disease, the mortality rate of severe acute pancreatitis is still 20%–30%.[3,4] Therefore, to assist physicians in clinical decision-making, by describing a range of generally acceptable approaches for the diagnosis and management of acute pancreatitis, and to inform patients and families about these approaches, the Japanese Society of Emergency Abdominal Medicine

(JSEAM) has contributed to producing practice guidelines for the disease. The Working Group for the Practical Guidelines for Acute Pancreatitis of the JSEAM systematically reviews the literature and directs evidence-based practical guidelines, with indications of levels of evidence in the literature and grades of recommendations (hereafter, grade) for interventions. The guidelines are supported and funded by the JSEAM.

These guidelines attempt to define practices that meet the needs of most patients in most circumstances. The ultimate judgment regarding care of a particular patient must be made by the physician and patient in light of all of the circumstances presented by that patient.

The guidelines were presented for discussion at the JSEAM meetings in 2001 and 2002, and on the internet homepage. These guidelines will be approved by JSEAM in 2002 and published in the journal of the JSEAM and updated on the JSEAM internet homepage (http://plaza.umin.ac.jp/~jaem/). Therefore, in this article, we will describe the process of the formation of the guidelines, the algorithms, and a brief summary of recommendations in the guidelines.

Process of formation of guidelines

MEDLINE (1960–2000) was searched with the MeSH (explode) terms "pancreatitis", "acute necrotizing pancreatitis", and "alcoholic pancreatitis" and the key word "pancreatitis". Over 28000 papers were searched for these terms, limited to human studies and those reported in English or Japanese, and 14821 papers were listed. Japana Centra Revuo Medicina (1991–2000) was also searched, with "pancreatitis" as the key word. In this way, 1475 papers were listed. Thus, a total of 16296 papers were selected, and 1348 papers and reports of the Working Group for Acute Pancreatitis of the Japanese Ministry of Health were reviewed and assessed according to the levels of evidence and grades of recommendations of the Oxford Centre for Evidence-Based Medicine (Table 1).[5] Practical recommendations were also graded according to suggestions in a previous report (Table 2).[6]

The guidelines were presented on the JSEAM homepage, and opinions were collected via the internet. After each presentation and discussion at the JSEAM meetings in both 2001 and 2002, the Working Group for the Practical Guidelines for Acute Pancreatitis modified these guidelines based on these collected opinions. The guidelines are still under development and will be approved by the JSEAM in 2002. The content and evidence base of the guidelines will be reviewed in 4 years' time.

Summary of the practice guidelines

The guidelines consist of introductions, a summary of recommendations (Table 3), practice algorithms (Figs. 1–6), definitions, epidemiology, diagnosis, severity assessment, and therapy. The main points are easily understood using practice algorithms and the summary of recommendations.

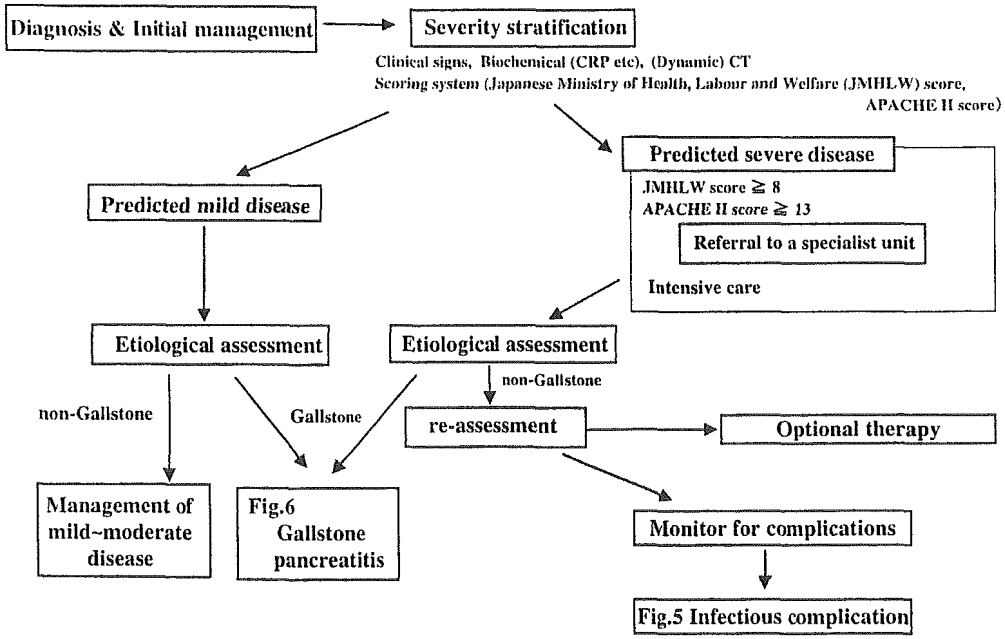

Fig. 1. Summary of management steps in acute pancreatitis. *CRP*, C-reactive protein; *CT*, computed tomography; *APACHE*, Acute Physiology and Chronic Health Evaluation

Table 1. Levels of evidence: 23 November, 1999 (http://cebm.jr2.ox.ac.uk/docs/levels.html)

Level of evidence	Therapy/prevention, Etiology/harm	Prognosis	Diagnosis	Economic analysis
1a	SR (with homogeneity[a]) of RCTs	SR (with homogeneity[a]) of inception cohort studies; or a CPG validated on a test set	SR (with homogeneity[a]) of level 1 diagnostic studies; or a CPG validated on a test set	SR (with homogeneity[a]) of level 1 economic studies
1b	Individual RCT (with narrow confidence interval[b])	Individual inception cohort study with ≥80% follow-up	Independent blind comparison of an appropriate spectrum of consecutive patients, all of whom have undergone both the diagnostic test and the reference standard	Analysis comparing all (critically validated) alternative outcomes against appropriate cost measurement, and including a sensitivity analysis incorporating clinically sensible variations in important variables
1c	All or none[c]	All or none case-series[d]	Absolute SpPins and SnNouts[e]	Clearly as good or better[f], but cheaper Clearly as bad or worse, but more expensive Clearly better or worse at the same cost
2a	SR (with homogeneity[a]) of cohort studies	SR (with homogeneity[a]) of either retrospective cohort studies or untreated control groups in RCTs	SR (with homogeneity[a]) of level ≥2 diagnostic studies	SR (with homogeneity[a]) of level ≥2 economic studies
2b	Individual cohort study (including low-quality RCT; e.g., <80% follow-up) a test set	Retrospective cohort study or follow-up of untreated control patients in an RCT; or CPG not validated in non-consecutive patients, or	Any of: • Independent blind or objective comparison • Study performed in a set of analysis incorporating clinically confined to a narrow spectrum of study individuals (or both), all of whom have undergone both the diagnostic test and the reference standard • A diagnostic CPG not validated in a test set	Analysis comparing a limited number of alternative outcomes against appropriate cost measurement, and including a sensitivity sensible variations in important variables
2c	"Outcomes" research	"Outcomes" research		
3a	SR (with homogeneity[a]) of case-control studies			
3b	Individual case-control study		Independent blind comparison of an appropriate spectrum, but the reference standard was not applied to all study patients	Analysis without accurate cost measurement, but including a sensitivity analysis incorporating clinically sensible variation in important variables